CHANGES IN DYNAMICS OF PENSILUNGPA GLACIER, WESTERN HIMALAYA, OVER THE PAST TWO DECADES

Aparna Shukla[1], Purushottam Kumar Garg[2,3], Manish Mehta[1], Vinit Kumar[1]
[1]Wadia Institute of Himalayan Geology, 33 GMS Road, Dehradun – 248001
[2]Center for Glaciology, Wadia Institute of Himalayan Geology, 33 GMS Road, Dehradun – 248001
[3] Post Graduate Department of Remote Sensing and GIS, University of Jammu, Jammu - 18006
Email: aparna@wihg.res.in

KEYWORDS: Glacier health, Glacier dynamics, Climate change, Supraglacial debris, western Himalaya

ABSTRACT:

The health of Himalayan glaciers has been a cause of prime concern for the scientific community as well as policy makers. The state of glacier dynamics is considered a significant indicator of glacier health. Surface ice velocity (SIV) is one of the important parameters which determines the glacier dynamics. The SIV is driven by several factors which include changes in hypsometry and slope, mass load, orientation of the glacier, basal sliding, debris cover and the variation in meteorological parameters. Further, as remote and inaccessible location of mountain glaciers inhibits their field based monitoring, remote sensing with repeat and synoptic coverage offers the best alternative. In present study, we have used multi-temporal satellite images from Landsat Thematic Mapper (TM), Enhance Thematic Mapper (ETM+) and Operational Land Imager (OLI) sensors for past two decades (1993/94 - 2016/17) to ascertain the variations in the SIV of the Pensilungpa glacier, Suru sub-basin, western Himalaya. For estimation of glacier velocity, the standard procedures using image to image cross-correlation technique have been employed. Results reveal that the mean glacier wide SIVs in the accumulation zone (ACZ) of the glacier have been decreasing, those in the upper ablation zone (ABZ) have been stable and even increasing, while the lower ABZ exhibits a slowdown. This slowdown may be linked with consistent increase (~ 40% in past 23 years) in the supraglacial debris cover extents on the glacier. The spatio-temporal pattern of fluctuations in the SIV of the glacier seem to be controlled primarily by variations in the regional meteorology, glacier mass balance and debris cover extent.

1. INTRODUCTION

Glaciers are the most critical natural resources constituting the Cryosphere. Population inhabiting the three major river basins (Indus, Ganga and Brahmaputra) in the Himalayan region, amounting to ~ 0.75 billion, rely on snow and glacier-melt waters for drinking, agriculture and power generation to varying extents (Immerzeel et al., 2010; Bolch et al., 2012; Hasson et al., 2014). Thus, repeated and comprehensive assessment of the status of Himalayan glaciers holds prime importance. Even as the recent remote sensing studies based on geodetic method and satellite laser altimetry data have shown a diverse spatial distribution of glacier mass changes in Himalayan Karakoram Tibet region (Gardelle et al., 2013; Kääb et al., 2015; Brun et al., 2017), details about the glaciers' specific response to climate change are scarce. This is primarily because glaciers mostly occur in remote locations making in situ measurements of glacier parameters specially glacier mass balance labour intensive, difficult and costly. This restricts a systematic assessment of the prevailing specific mass balance trends which in turn hampers monitoring of glacier health. Alternatively, remote-sensing based glacier surface ice velocities (SIV) may be used as indicators of glacier conditions (Scherler et al., 2011a).

The velocity field of a glacier is an important glaciological parameter that governs a variety of processes, and controls glacier geometry and extent (GLIMS book). The SIV is the sum of glacier flow as a result of (i) shear deformation and (ii) basal sliding. Also, slope gradient, bedrock characteristic, and meltwater availability can also affect the movement of the glaciers to varying extents (Garg et al., 2017). The SIV may vary intra-annually (seasonally) as well as inter-annually. In general, as the ablation period sets in, released meltwater enhances the basal sliding and hence the SIV. Thus, the maximum SIV may be found during the peak ablation period, which again decreases as the ablation period ends (Scherler and Strecker, 2012). Glacier ice velocity measurement done in field usually have a poor spatial coverage owing to various problems, contrary to which, the remote sensing based estimates are spatially more robust. Presently, three methods are commonly used for estimation of glacier SIV, these include synthetic aperture radar (SAR) interferometry, SAR tracking techniques, and cross correlation of optical satellite images. SIV measurements by InSAR are most appropriate for analyzing very short time scales, i.e., days, or where extrapolation to longer time scales is justified, e.g., in ice sheet studies (Joughin et al., 2002). Feature tracking, using SAR or optical imagery is more appropriate for analyses over longer periods. Although limited by cloud cover during image acquisition, cross correlation of optical imagery provides a quick and efficient way of measuring glacier surface velocities (Scherler et al., 2008).

Considering the above, in this paper, variation in dynamics of the Pensilungpa glacier, Suru sub-basin, western Himalaya, over past two decades (1993/94 to 2016/17) has been assessed using cross-correlation technique on Landsat image pairs of different time periods. The SIV variations of the glacier have been analysed with respect to changing meteorological (temperature and precipitation) and other glacier parameters (e.g. debris cover and snow line altitude (SLA)).

2. STUDY AREA

The Pensilungpa glacier is a medium sized (~8 km) compound valley-type glacier formed by coalition of three tributary glaciers and is situated near the Pensi La pass, sometimes called the 'Gateway to Ladakh' (Kamp et al., 2011) (Figure 1). This glacier is the source of the Suru River which flows northwest and meets the Indus River near Chathantag (2535 m asl). The Suru basin supports 284 glaciers with 719 km^2 glacierized area. The study area may be described as a high-altitude semi-desert lying on the northern flank of the Great Himalayan Range. This mountain range acts as a climatic barrier shielding the area from most of the monsoon and creates a rain shadow zone. The region receives snowfall during winter due to western disturbances and rainfall during the summer (Shukla and Qadir, 2016).

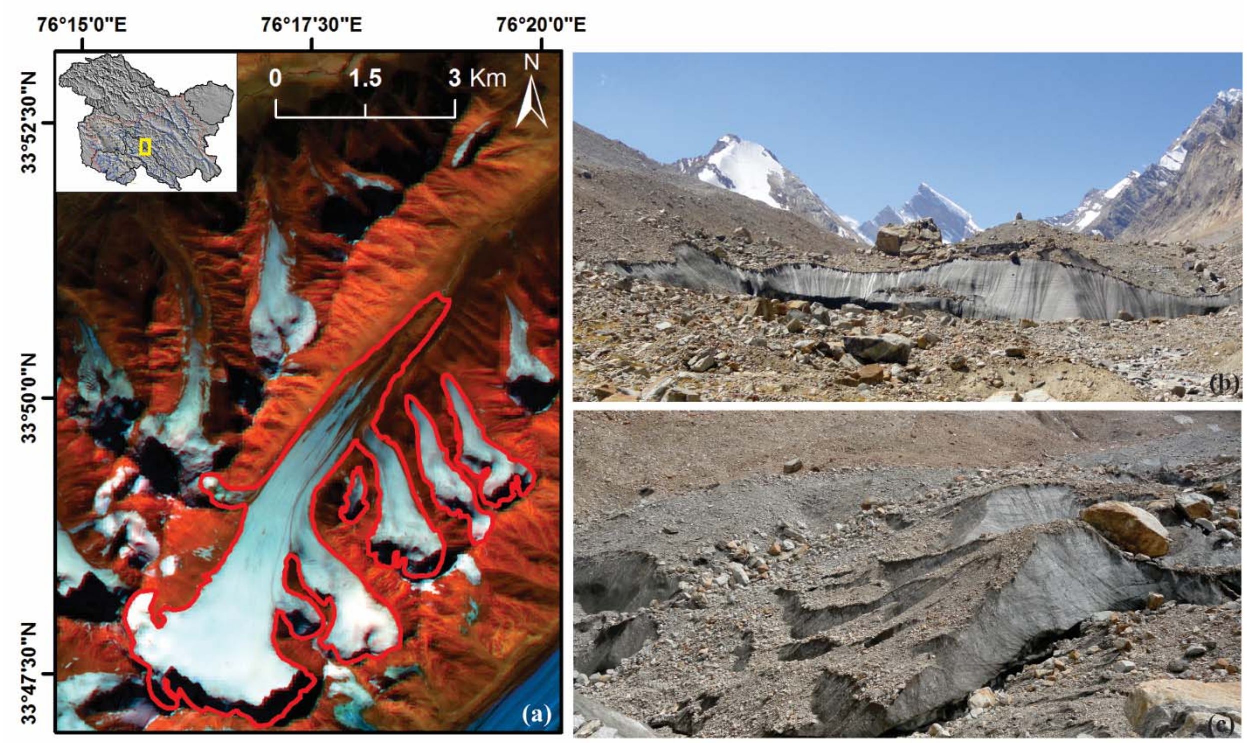

Figure 1. Location map and geomorphology of the study area. **(a)** A false colour composite (FCC, R=Short wave Infrared band, G= Near Infrared band, B= Blue band) generated from the 25 October 2016 Sentinel-2 MSI image of the study area. Red polygon depicts the glacier boundary. **(b)** Field photograph of the glacier snout taken in September 2016. Note the extensive debris cover on the snout and high (~22 m) ice wall. **(c)** Field photograph showing the heavily crevassed surface of the glacier with heterogeneous debris cover and exposed ice-cliffs.

3. DATA SETS AND METHODS

The SIV for the period of 1993/94, 1999/2000 and 2016/17 were obtained using Landsat image pairs (Near infrared band). The pre and post event images were selected in such fashion that they have about one year temporal separation (Table 1). The orthorectification, precise co-registration and sub-pixel correlation of image pair constitute the important steps of displacement computation. For this, we acquired all the selected TM, ETM+ and OLI images as orthorectified in the processing level L1T. Further, given the same acquisition geometry (orbit, pointing angle, etc.) of Landsat image pair, simple co-registration was found to be sufficient to account for offsets between the repeated images and achieve precise congruence (Kaab et al., 2005). Subsequently, the correlation of image pair was performed using Coregistration of Optically Sensed Images and Correlation (COSI-Corr), an add-on module of ENVI software (Leprince et al. 2007; Tiwari et al., 2014) using a window size of 64 down to 32 pixels. Steps of 2 pixels between adjacent correlations yielded ice flow velocity maps sampled at every 60 m (Scherler et al., 2008). The correlation produced displacement maps in north-south (NS) and east west (EW) directions along with a signal-to-noise ratio (SNR) that defines confidence of the results. During the post processing, low SNR points were filtered out to eliminate poorly correlated pixels. Also, to remove points that do not match with the general flow pattern of glacier, a directional filter was applied (Scherler et al., 2008; Scherler and Strecker, 2012; Garg et al., 2017). Finally, the velocity was computed as per the following:

$$SIV = \sqrt{NS^2 + EW^2} \quad (1)$$

Additionally, the SIV >60 m/y was also filtered out to eliminate any miscorrelated pixel. Lastly, to simplify the results, all the velocity products were normalized for 365 days interval (i.e. m/y). The SIV were assessed along the central flow line of the glacier, averaged over every 300 m distance from the snout.

Table 1. List of image pairs used for velocity estimation.

Platform Sensor	**Scene ID**	**Date of acquisition**	**Spatial resolution**	**Specification**
Landsat-5 TM	LT51480371993236ISP00	24-08-1993	30	Pre event image 1
Landsat-5 TM	LT51480371994207ISP00	26-07-1994	30	Post event image 1
Landsat-7 ETM+	LE71480371999229AGS00	17-08-1999	30	Pre event image 2
Landsat-7 ETM+	LE71480372000248SGS00	04-09-2000	30	Post event image 2
Landsat-8 OLI	LC81480372016252LGN00	08-09-2016	30	Pre event image 3
Landsat-8 OLI	LC81480372017206LGN00	25-07-2017	30	Post event image 3

The uncertainties in the annual velocities were computed over stable areas following Scherler and Strecker (2012). This involves adding the mean and standard deviation of the total displacement uncertainties and dividing by the temporal separation of the correlated images. Table 2 presents the uncertainty estimation statistics for all the three time periods considered in this study.

Table 2. Statistics of uncertainty estimation of surface ice velocity (SIV).

Time period	**No of non-glaciated (ng) pixels considered (*n*)**	**Mean SIV** (SIV_{mng_mean})	**Standard deviation** (SIV_{ng_STDEV})	**Total uncertainty in SIV** ($E_{SIV} = SIV_{ng\_mean} + SIV_{ng\_STDEV}$)
1993/94	32555	3.86	2.12	5.98
1999/2000	48891	2.52	1.46	3.98
2016/17	8302	3.96	2.07	6.03

Temporal variation in SIV of the glacier were analysed with respect to the changes in meteorological variables over the study duration. The temperature and precipitation data for past 25 years (1990 to 2015) was derived from the Climate Research Unit (CRU) TS 4.0 dataset (Figure 2). It is a gridded (0.5° x 0.5°) climate dataset (referred to as CRU TS 4.0) from monthly observations at meteorological stations across the world's land areas (Harris et al., 2013).

Besides, changes in SIV were also compared with debris cover changes and SLA variations. Debris cover was mapped manually on the images of respective time periods (Table 1) for deriving the spatio-temporal changes. For estimating the SLA, first, the snowlines were mapped taking advantage of the differences in reflectance of snow and ice. Thereafter, altitude along the snowline was extracted from the Shuttle Radar Topographic Mission (SRTM) Global Digital Elevation Model version-3 (GDEM-v3) using 30 m (15 m either side of the lines) buffer around the digitized snow lines (along with standard deviation; SD) (Shukla and Qadir, 2016; Garg et al., 2017).

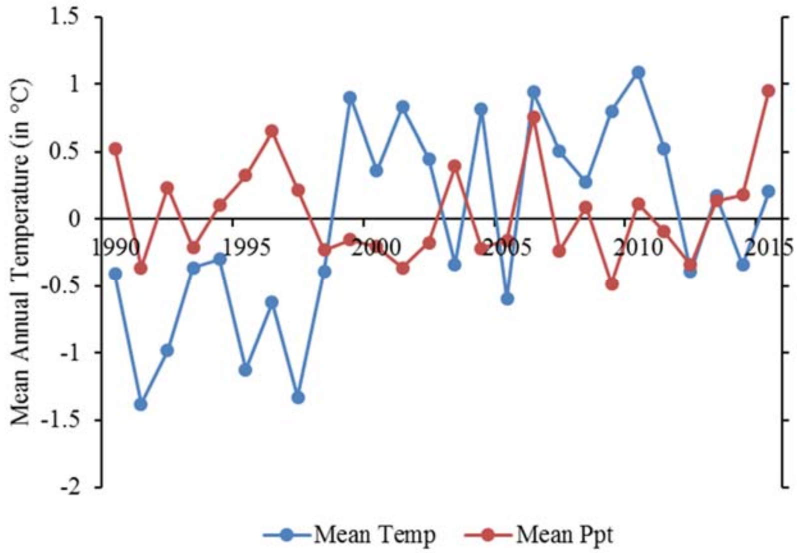

Figure 2. Temperature and precipitation variability in the study area for past 25 years (1990-2015) derived from the CRU TS 4.0 dataset.

4. RESULTS AND DISCUSSION

Analysis of the temporal SIV changes of the Pensilungpa glacier reveals a highly fluctuating trend (Figure 3 and 4). The mean glacier wide SIV first decreased from 16.29 m yr^{-1} in 1993/94 to 12.32 m yr^{-1} in 1999/00, registering a slowdown of ~24% (Figure 3). However, from 1999/00 to 2016/17 a considerable acceleration (~ 30%) was observed as the SIV regained to 16.08 m yr^{-1} in 2016/17. Further, a slight increase in SIV even in the lower ablation areas (Figure 3) between 1999/2000 and 2016/17 clearly indicate that all the glacier parts are active throughout the tongue. Besides, it may be noted that while the SIV curves for year 1993/94 and 2016/17 appear more or less similar, the velocity profile for 1999/00 shows consistently lower values (Figure 3).

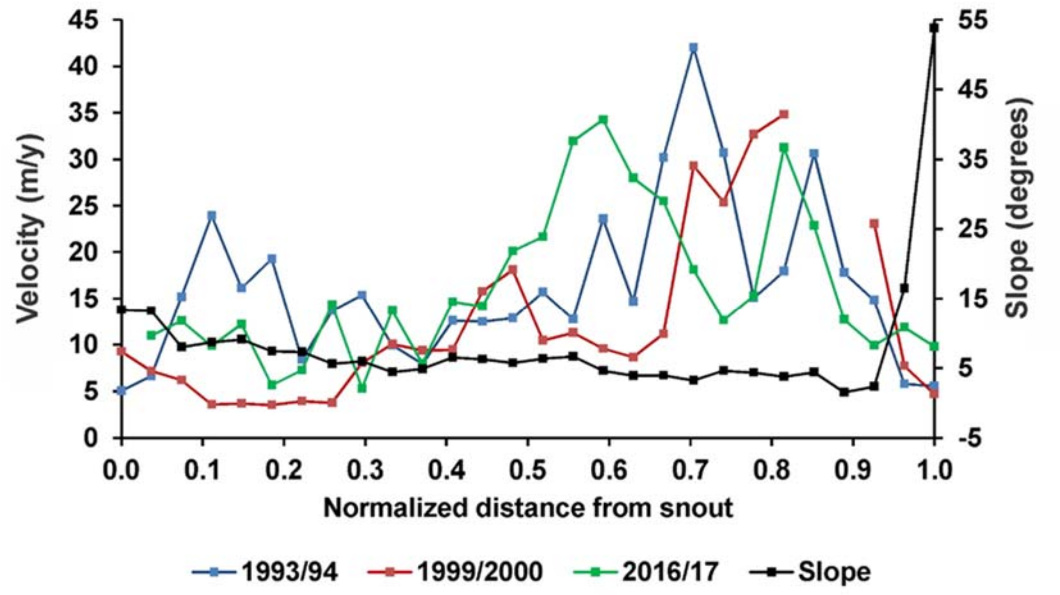

Figure 3. Surface ice velocity (SIV) of Pensilungpa glacier computed along the central flow lines and averaged over every 300 m distance from snout.

Further, interesting spatial trends are observed while assessing the zone-wise SIV variations of the glacier. It is observed that SIVs in the accumulation zone (ACZ) of the glacier have been steadily declining. The mean velocity of the ACZ decreased from 20.71 m yr^{-1} in 1993/94 to 19.71 m yr^{-1} in 1999/00 and further to 17.98 m yr^{-1} in 2016/17.While the mean velocity on the ablation zone (ABZ) of the glacier was found to have first decreased from 12.98 m yr^{-1} in 1993/94 to a low of 8.41 m yr^{-1} in 1999/00, which subsequently increased to 14.77 m yr^{-1} in 2016/17. This reveals that over the past two decades, while the SIV in the ACZ of the glacier declined (~ 13%), the ABZ rejuvenated dynamically exhibiting an increase in SIV by ~14%. Another, interesting observation regarding the change in dynamics of the glacier over past two decades appears to be that it is the upper ablation zone areas which exhibit increased SIVs while the lower ABZ region shows a slowdown (Figure 4), which may be linked with the debris cover increase.

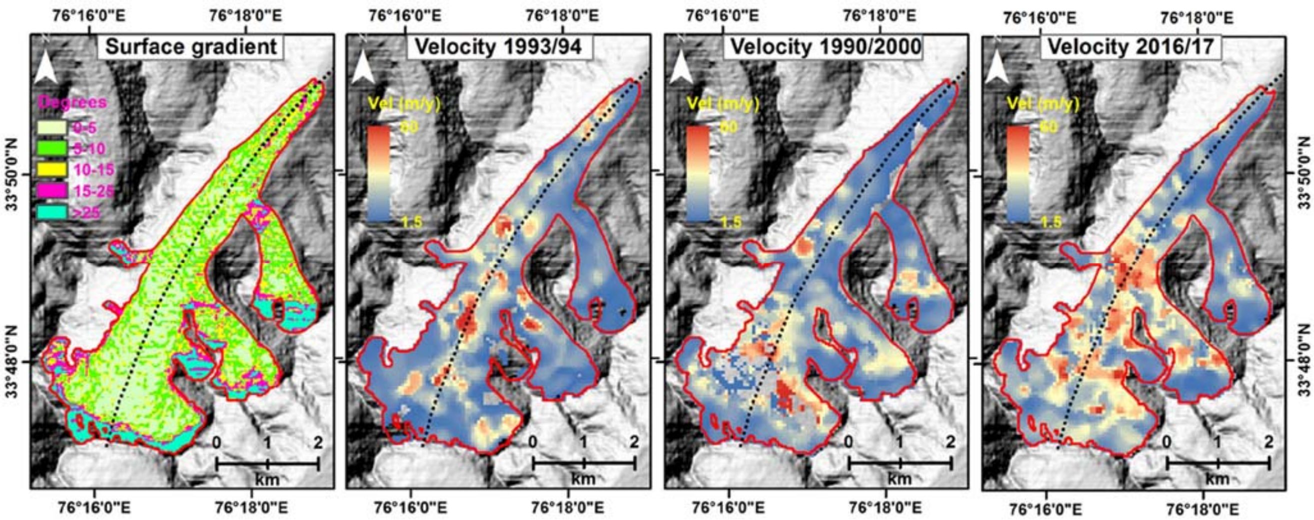

Figure 4. Spatial distribution of surface ice velocity (SIV) on Pensilungpa glacier for 1993/94, 1990/2000 and 2016/17 together with surface gradient map.

The SIV changes of the Pensilungpa glacier seem to be in-sync with the temperature and precipitation changes in the study area. In can be observed that while the mean temperature of the region has shown a secular increase over the past 25 years, however, there have been considerable fluctuations in the precipitation received by the area (Figure 2). The SIV changes of the glacier show a strong negative correlation (correlation coefficient (r) = −0.92) with the temperature changes and a stronger positive correlation ($r = 0.97$) with the precipitation variations. This reveals the strong influence of meteorological forcing factors on the temporal glacier SIV changes of the Pensilungpa glacier.

Comparing the SIV variations with the other glacier parameters it was found that while the mean glacier wide SIV changes were weakly sensitive to the debris cover increase ($r = -0.04$), they were fairly related with the SLA upshift ($r = -0.58$) in the region. Results show that during the study period, the supraglacial debris cover on the glacier has increased by ~ 40% (changing from 1.63 km^2 in 1993 to 2.28 km^2 in 2016). However, the SLA of the glacier has risen by ~153 m (increasing from 5035 m in 1993 to 5188 m in 2016). While the glacier wide SIV variations may show a weak sensitivity to the debris cover increase, however, the spatio-temporal changes in the SIVs reveal recent slowdown in the lower ablation region of the glacier (Figure 4). This is the part of the glacier which is heavily debris covered and this is where the debris cover extents have been increasing (Figure 1c). The supraglacial debris cover over the glacier ablation and terminus considerably affects the surface ice velocity by restricting its flow. Further, a fair relationship of the SIV changes with the SLA upshift clearly indicates the bearing of mass fluctuations on the dynamics of the glacier. Thus, noticeable slowdown of the glacier together with significant increase in supraglacial debris cover suggest a persistent mass loss scenario and indicates towards the negative health of the glacier.

The glacier is characterized by a gentle surface gradient (~< 10°; Figure 4) and hence the terrain slope and surface gradient changes seem to have a limited/secondary control on the spatial variation of the glacier SIV. The SIV of the Pensilungpa glacier, thus, seem to be primarily governed by the meteorological changes and mass fluctuation of the glacier.

5. CONCLUSION

The present study aimed at exploring the variations in dynamics of the Pensilungpa glacier, located in the Suru basin, western Himalaya using cross-correlation technique on multitemporal satellite images. Results revealed that from 1993/94 to 1999/00 the SIVs showed considerable slowdown, however, the average glacier velocity again normalized by 2016/17. The zone-wise analysis shows that while velocities in the ACZ have been consistently declining, those in the ABZ (upper part) have increased with time. The lower ABZ has shown a steady decrease probably due to debris cover increase. Variations in meteorological parameters, mass fluctuations and debris cover extents seem to be the major driving forces behind the dynamics of the Pensilungpa glacier.

REFERENCES

Bolch, T., Kulkarni, A., Kääb, A., Huggel, C., Paul, F., Cogley, J.G., Frey, H., Kargel, J.S., Fujita, K., Scheel, M., Bajracharya, S., 2012. The state and fate of Himalayan glaciers. Science, 336 (6079), pp. 310–314.

Brun, F., Berthier, E., Wagnon, P., Kääb, A., and Treichler, D.,. 2017. A spatially resolved estimate of High Mountain Asia glacier mass balances from 2000 to 2016. Nature Geoscience, pp. 1-7. DOI: 10.1038/NGEO2999.

Gardelle, J., Berthier, E., Arnaud, Y., and Kaab, A., 2013. Region-wide glacier mass balances over the Pamir-Karakoram-Himalaya during 1999-2011. The Cryosphere, 7(4), pp. 1263–1286.

Garg, P.K., Shukla, A., Tiwari, R.K., Jasrotia, A.S., 2017. Assessing the status of glaciers in part of the Chandra basin, Himachal Himalaya: a multiparametric approach. Geomorphology 284, pp. 99–114. http://dx.doi.org/10.1016/j.geomorph.2016.10.022.

Hasson, S., Lucarini, V., Khan, M. R., Petitta, M., Bolch, T., and Gioli, G., 2014. Early 21st century snow cover state over the western river basins of the Indus1 River system. Hydrology and Earth System Sciences, 18(10), pp. 4077–4100.

Immerzeel, W.W., van Beek, L.P.H., and Bierkens, M.F.P., 2010. Climate change will affect the Asian water towers. Science, 328, pp. 1382–1385

Joughin, I. (2002). Ice-sheet velocity mapping: a combined interferometric and speckle tracking approach. Annals of Glaciology, 34, pp. 195−201.

Kääb, A., 2005. Combination of SRTM3 and repeat ASTER data for deriving alpine glacier flow velocities in the Bhutan Himalaya. Remote Sens. Environ.94, pp. 463–474.

Kääb, A., Treichler, D., Nuth, C., Berthier, E., 2015. Brief communication: contend-ing estimates of 2003–2008 glacier mass balance over the Pamir–Karakoram–Himalaya. Cryosphere9 (2), pp. 557–564. http://dx.doi.org/10.5194/tc-9-557-2015.

Kamp, U., M. Byrne, and T. Bolch. 2011. "Glacier Fluctuations between 1975 and 2008 in the Greater Himalaya Range of Zanskar, Southern Ladakh." Journal of Mountain Sciences 8 (3), pp. 374–389. doi:10.1007/s11629-011-2007-9.

Leprince, S., Barbot, S., Ayoub, F., Avouac, J.P., 2007. Automatic and precise orthorectification, coregistration, and subpixel correlation of satellite images, application to ground deformation measurements. IEEE Trans. Geosci. Remote Sens. 45 (6), pp. 1529–1558.

Scherler, D., Strecker, M.R., 2012. Large surface velocity fluctuations of Biafo glacier, central Karakoram, at high spatial and temporal resolution from optical satellite images. J. Glaciol. 58 (209), pp. 569–580.

Scherler, D., Leprince, S., Strecker, M.R., 2008. Glacier-surface velocities in alpine terrain from optical satellite imagery—accuracy improvement and quality assessment. Remote Sens. Environ. 112 (10), pp. 3806–3819.

Scherler, D., Bookhagen, B., Strecker, M.R., 2011. Spatially variable response of Himalayan glaciers to climate change affected by debris cover. Nat. Geosci. 4 (3), pp. 156–159.

Shukla, A., Qadir, J., 2016. Differential response of glaciers with varying debris cover extent: evidence from changing glacier parameters. Int. J. Remote Sens. 37 (11), pp. 2453–2479.

Tiwari, R.K., Gupta, R.P., Arora, M.K., 2014. Estimation of surface ice velocity of Chhota- Shigri glacier using sub-pixel ASTER image correlation. Curr. Sci. 106 (6), pp. 853–859.